

P-Cygni Type Ly α from Starburst Galaxies

Sang-Hyeon Ahn,¹ Hee-Won Lee² and Hyung Mok Lee³

¹ *School of Physics, Korea Institute for Advanced Study, 207-43 Cheongyangri-dong, Dongdaemun-gu, Seoul, 130-012, Korea*

² *Department of Geoinformation Sciences, Sejong University, Seoul 143-747, Korea*

³ *School of Earth and Environmental Sciences, Astronomy Program, Seoul National University, Seoul 151-742, Korea.*

Submitted version, 29 Mar 2002

ABSTRACT

P-Cygni type Ly α profiles exhibited in nearly half of starburst galaxies, both nearby and high- z , are believed to be formed by an expanding supershell surrounding a star-forming region. We apply the Monte Carlo code which was developed previously for static and plane-parallel medium to calculate the Ly α line transfer in a supershell of neutral hydrogen which are expanding radially in a spherical bulk flow. We consider typical cases that the supershell has the Ly α line-centre optical depth of $\tau_0 = 10^5 - 10^7$, a radial expansion velocity of $V_{\text{exp}} \sim 300 \text{ km s}^{-1}$, and the turbulence of $b \simeq 40 \text{ km s}^{-1}$. We find that there appear a few emission peaks at the frequencies corresponding to $(2N - 1)V_{\text{exp}}$, where the order of back scatterings $N > 1$. As $V_{\text{exp}} \rightarrow b$, the emergent profiles become similar to those for the static medium and the peaks are less prominent. We also investigate the effects of column density of the supershell on the emergent Ly α profiles. We find that the number and the flux ratios of emission peaks are determined by interplay of τ_0 and V_{exp} of the supershell. We discuss the effects of dust extinction and the implication of our works in relation to recent spectroscopic observations of starburst galaxies.

Key words: line: formation — radiative transfer — galaxies: starburst — galaxy: formation

1 INTRODUCTION

Ly α emission lines render us a very useful redshift indicator for starburst galaxies at high redshift, because their rest-frame equivalent width was predicted to be $50 - 200 \text{ \AA}$ (Charlot & Fall 1993). Thommes et al. (1998) suggested that the existence of strong Ly α emission is a

necessary condition for primeval galaxies. However, dust enrichment is believed to be a fast process in the early evolution of galaxies, and therefore Ly α should suffer severe extinction by dust. It has been argued that even a small amount of dust in a very thick hydrogen medium can destroy Ly α photons because their path lengths before escape increase tremendously due to a huge number of resonance scatterings. Hence, dust absorption is believed to be the main reason for the early null detection of Ly α emission from high- z galaxies by narrow band imaging surveys.

The Lyman break method has been very successful among a few programs to detect high- z galaxies. Steidel et al. (1996) presented the rest-frame UV spectra of primeval galaxies at $\langle z \rangle = 3$. They continued to search for even more distant galaxies, and secured the spectra of galaxies at the redshift $\langle z \rangle = 4$ (Steidel et al. 1999). The UV spectra of those primeval galaxies are characterized by a flat UV continuum and the three types of the Ly α feature: symmetric emission, broad absorption in the wings, and P-Cygni type asymmetric emission.

From *HST GHRS* observations of nearby H II galaxies, Kunth et al. (1998) discovered that P-Cygni type Ly α emission lines are always accompanied by the low-ionization interstellar absorption lines blueshifted by 100–300 km s $^{-1}$ with respect to the systemic velocity, while broad wing absorptions of Ly α are accompanied by the much less blueshifted interstellar absorption lines. There are spectral similarities between nearby and high- z starburst galaxies. Recently there have been a number of observations to obtain rest-frame optical nebular lines from high- z galaxies (Teplitz et al. 2000a; Teplitz et al. 2000b; Pettini et al. 2001).

These observations support the idea that the kinematics of surrounding media plays a crucial role in the survival of Ly α photons in primeval galaxies, which is similar to the case in nearby starburst galaxies. When the systemic redshifts were determined by using the nebular lines, evidence for bulk motions of several hundred km s $^{-1}$ is found (Pettini et al. 2001). Ahn & Lee (1998) and Lee & Ahn (1998) investigated the formation of asymmetric Ly α line profiles observed in the spectra of high- z galaxies by introducing the galactic superwind model.

It is generally believed that the Ly α emission is not a good indicator for the star-formation rate, because of dust extinction. However, Ly α emission often bears a nearly unique information on high- z starburst galaxies. Therefore, we have to understand the line formation mechanism, in order to establish the quantitative measure of star-formation rate.

We have been investigating the Ly α line formation in thick and static media of neutral

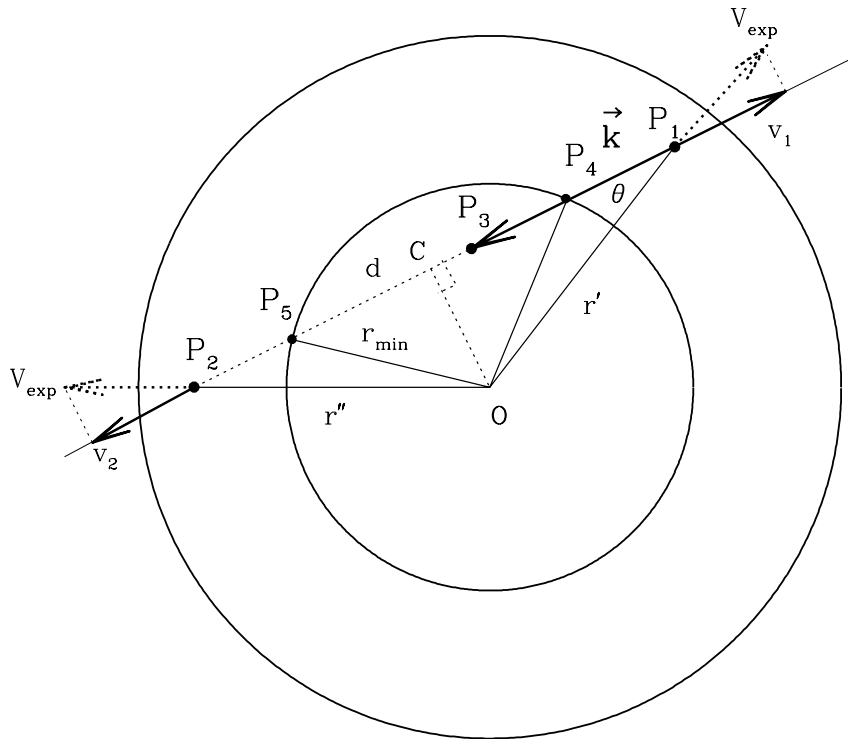


Figure 1. Schematic diagram for the back-scattered photons. Here a Ly α photon would propagate from P₁ to P₃. However, because the central region is devoid of neutral hydrogen, the photon traverse freely to P₂, which is receding with respect to the photon. Details are explained in the text.

hydrogen, and developed an accurate and efficient Monte Carlo method (Ahn, Lee, & Lee 2000, 2001, 2002). In this paper we apply our method to an expanding spherical supershell. In section 2 we describe our Monte Carlo code. We show the detailed mechanism of Ly α line transfer in expanding media in section 3, and the effects of both thickness and expansion velocity of the supershell in section 4. In the last section we summarize the results and discuss on the implication of our works.

2 MONTE CARLO METHOD

Our model for starburst galaxies is illustrated in Figure 1. We assume that there is a central star-forming region surrounded by an expanding spherical supershell. We also assume that

the Ly α source is the central super star cluster, because the Ly α luminosity of a typical starburst galaxy is equivalent to ionizing photons from $10^3 - 10^4$ O, B stars (González Delgado 1998; Ahn 2000) and the star-forming region is compact (Frye et al. 2002).

Expanding supershells are frequently seen in nearby starburst galaxies in a kiloparsec scale around the central star-forming region (Marlowe et al. 1995; Martin 1998). Recent *HST* observations revealed that the neutral column density of a supershell ranges $N_{\text{HI}} \sim 10^{18} - 10^{22} \text{ cm}^{-2}$, which is deduced from usual Voigt fitting analyses (Kunth et al. 1998). The Ly α line-centre optical depth is related with the H I column density N_{HI} by

$$\tau_0 \equiv 1.41 \left(\frac{b}{12.9 \text{ km s}^{-1}} \right)^{-1} \left[\frac{N_{\text{HI}}}{10^{13} \text{ cm}^{-2}} \right], \quad (1)$$

where b is the Doppler width for turbulence motion. Therefore, we should deal with scattering media with the line-centre optical depths $\tau_0 = 10^5 - 10^9$. However, Monte Carlo methods are usually inefficient in this regime, because of the large computing time due to the large number of resonance scatterings required before escape. Hence we developed an accelerated Monte Carlo method in the previous paper (Ahn, Lee, & Lee 2002).

In an expanding supershell, some photons are scattered back into the opposite part of the supershell, and so they get redshifted. They experience a series of such back-scatterings before they escape the system. These processes enhance the escape probability of Ly α resonance photons in optically thick media than in static medium, and the number of scatterings before escape becomes much less than that in static media. Therefore, even though we want to solve the problem of radiative transfer in extremely thick media, it is sufficient for us to use the original code described in Ahn et al. (2001).

We illustrate the back-scattering process in Figure 1. Suppose that a photon scattered at P_1 to a direction $\mathbf{k} \parallel \overrightarrow{P_1 P_3}$ is scattered at a next scattering site P_3 if the central region is also uniformly filled with neutral hydrogen atoms. Since no neutral hydrogen is assumed to be present in $\overline{P_4 P_5}$, the photon traverses to P_2 , where $|\overline{P_5 P_2}| = |\overline{P_4 P_3}|$. We determine the distance $2d \equiv |\overline{P_4 P_5}|$ along the wave vector \mathbf{k} , and add $|\overline{P_4 P_5}|$ to the path length $|\overline{P_1 P_3}|$ in the code. Here we define the position vectors of the adjacent scatterings to be \mathbf{r}' and \mathbf{r}'' , $r' = |\mathbf{r}'|$, and the angle $\theta \equiv \angle OP_1 P_4$. An elementary geometrical calculation gives

$$d = r' \cos \theta - l, \quad (2)$$

where

$$\cos \theta = -\frac{\mathbf{r}' \cdot \mathbf{k}}{|\mathbf{r}'|}, \quad (3)$$

$l \equiv |\overline{P_1P_4}| = r' \cos \theta - [r'^2 \cos^2 \theta - r'^2 + r_{min}^2]^{1/2}$, and $|\overline{OP_4}| = |\overline{OP_5}| \equiv r_{min}$.

The velocity shifts due to the bulk expansion of the medium should be taken into account. Referring to the geometry shown in Figure 1, the velocities \mathbf{v}_1 and \mathbf{v}_2 are given by

$$\mathbf{v}_1 = -V_{\text{exp}} \cos \theta \mathbf{k}, \tag{4}$$

and

$$\mathbf{v}_2 = V_{\text{exp}} \frac{s - l + d}{r''} \mathbf{k}, \tag{5}$$

where V_{exp} is the expansion velocity of the supershell and $V_{\text{exp}} > 0$ by definition. Here $s \equiv |\overline{P_1P_3}|$ is the path length corresponding to an optical depth $\tau = -\ln R$, where $R \in [0, 1]$ is a random number. We subtract frequency corresponding to the relative velocity $\Delta \mathbf{v} = \mathbf{v}_2 - \mathbf{v}_1$ from the frequency x whenever a back-scattering occurs. Here we introduce the dimensionless frequency parameter x defined by

$$x \equiv \frac{\Delta \nu}{\Delta \nu_D} = \frac{(\nu - \nu_0)}{\Delta \nu_D}, \tag{6}$$

which describes the frequency shift from the line-centre frequency ν_0 in units of the Doppler width $\Delta \nu_D \equiv \nu_0(b/c)$. Here b is the Doppler parameter that combines both turbulence and the thermal motions of the scattering medium, and c is the speed of light. The detailed description of our code can be found in the previous papers (Ahn, Lee, & Lee 2000, 2001, 2002).

While scatterings occur in the supershell, we should also take into account the Doppler shift caused by the relative bulk motion between the two adjacent scattering positions. For the radial vectors of the adjacent scattering locations, \mathbf{r}_1 and \mathbf{r}_2 , the expansion velocities projected into the wave vector should be considered. After a simple geometrical consideration, we obtain

$$\Delta v = V_{\text{exp}} \left(\frac{\mathbf{r}_2}{|\mathbf{r}_2|} - \frac{\mathbf{r}_1}{|\mathbf{r}_1|} \right) \cdot \mathbf{k}. \tag{7}$$

We subtract this shift from the frequency of a Ly α photon whenever scatterings take place in the medium. When a Ly α photon escapes the medium by a back-scattering, we consider the redshifts due to the final back-scattering; i.e., only \mathbf{v}_1 in Eq.(4) is taken into account. We also calculate the path lengths of photons traversing in the supershell in order to estimate the amount of dust extinction. However, dust effect is considered very briefly in this paper, and we will concentrate on the Ly α line transfer in the expanding supershell.

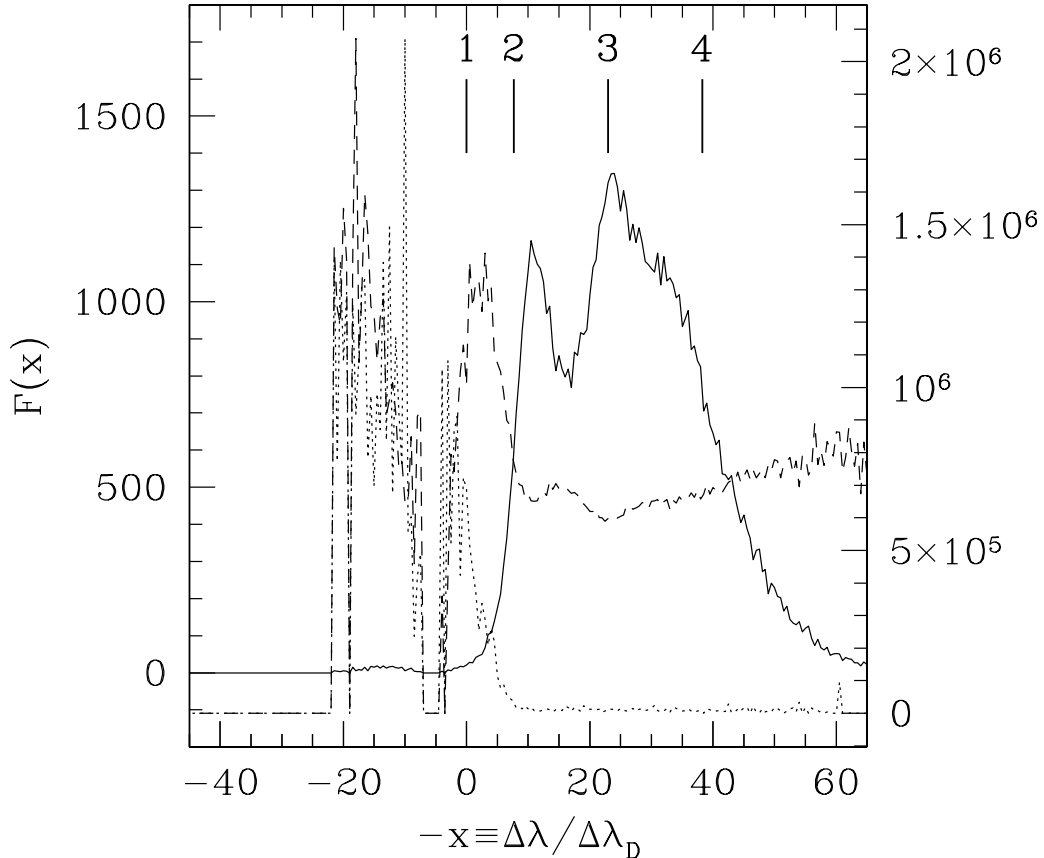


Figure 2. An emergent profile (solid line) of Ly α emission calculated by our Monte Carlo code. The dashed line represents the total number of scatterings before escape, and the dotted line refers to the number of successive wing scatterings just before escape. The horizontal axis refers to the wavelength shift in units of thermal width. The right vertical axis refers to the number of scatterings, and the left one refers to the number flux of the emergent spectrum. The vertical lines with numbers in the box indicate the frequencies of possible emission peaks. See the model parameters in the text.

3 THE FORMATION OF P-CYGNI TYPE LY α PROFILES

We now discuss on typical profiles of Ly α resulting from the scattering processes discussed above. The expanding supershells in starburst galaxies have typical turbulence which is given by the Doppler parameter, $b \simeq 40 \text{ km s}^{-1}$ estimated from Voigt fittings (*e.g.* Kunth et al. 1998). Hence we assume that the Voigt parameter of the expanding supershell to be $a = 1.5 \times 10^{-4}(40 \text{ km s}^{-1}/b)$, where the Voigt parameter $a \equiv \Gamma/4\pi\Delta\nu_D$ with Γ being damping constant. Here we neglect the thermal motion, because the turbulent motion usually exceeds the thermal motion. The FWHM of the input profiles is set to be $\Delta x = 2$, because the optical nebular emission lines indicate that $\Delta v = 70 \sim 100 \text{ km s}^{-1}$ (Pettini et al. 2001). We consider a supershell with its expansion velocity being $V_{\text{exp}} \sim 300 \text{ km s}^{-1}$ and its column

density $10^{18} \text{ cm}^{-2} < N_{\text{HI}} < 10^{21} \text{ cm}^{-2}$, in accordance with observations in nearby starbursts (Kunth et al. 1998) and high- z galaxies (Pettini et al. 2001). These two quantities satisfy the condition $a\tilde{\tau}_0 > 10^3$, which guarantees the validity of the analytic solution given by Adams (1972), Harrington (1973), and Neufeld (1990). Here we define the line centre-optical depth by $\tilde{\tau}_0 \equiv \sqrt{\pi}\tau_0$, which is a little bit different from the previous researches.

In Figure 2 we show the emergent profile for the model. The number of photons used in the Monte Carlo calculation is 80,000, and the other physical parameters are assumed to be the typical values mentioned above. Especially we choose the neutral column density $N_{\text{HI}} = 2 \times 10^{20} \text{ cm}^{-2}$. The dotted line in the figure represents the average number of scatterings for a photon during its transfer, and the dashed line represents the average number of successive wing scatterings just before its escape. The solid line refers to the emergent Ly α profile. The vertical bars with numbers refer to the frequency of emission peaks corresponding to N -th back-scattering. We can see two kinds of peaks in the profile: one located at the bluer frequency, and the other three at the redder part.

We see in the figure that the weak peak at the blue part is composed of photons which have experienced very large number of scatterings in the wings as well as in the core. According to Adams (1972), the number of scatterings for those photons is $N \propto \tau_0$. Hence we can see that these are photons transferred in the supershell by so-called excursions (Adams 1972). Some photons around $x \simeq 0$ are also similar ones, which is evident by the large number of scatterings and wing scatterings.

These weak peaks are formed through the following processes. When photons with the line-centre frequency are incident upon the inner wall of the expanding supershell, its scattering is off-centred by an amount of x_{exp} , where we define the dimensionless frequency corresponding to the expansion velocity $x_{\text{exp}} \equiv -V_{\text{exp}}/v_{\text{th}}$. Hence, the fraction of transmitted photons through the supershell is approximately given by Eq.(2.23) in Neufeld (1990), and the profile of transmitted photons is given by Eq. (2.32) in the same paper. Since $x_{\text{exp}} = -7.65$ in the above simulation, we can see from Eq.(2.23) in Neufeld (1990) that a very small amount of photons can transmit the optically very thick supershell and majority of photons are back-scattered. The transmitted photons are redistributed into both sides of $x = -x_{\text{exp}}$. The radiative transfer of those photons was studied very well both analytically (Neufeld 1990) and numerically (Ahn et al. 2002).

The three peaks at the red part are composed of back-scattered photons. Since the supershell is receding with respect to the incident photon, scatterings usually occur at wing

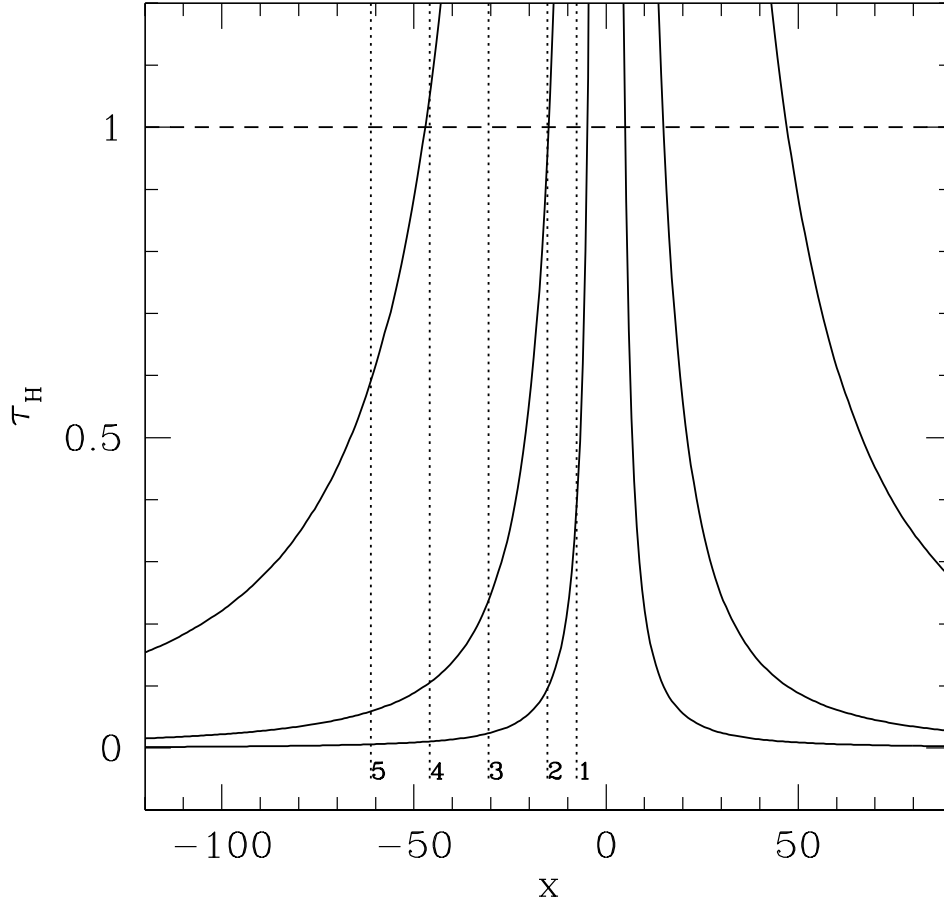


Figure 3. Ly α scattering opacity for the cases with the line-centre optical depths of $\tau_0 = 10^5, 10^6, 10^7$, which are drawn by solid lines from the innermost one. The vertical dotted lines represent the effective scattering frequencies, and the number refers to the order of back-scattering with atoms in the supershell.

frequencies if the opacity at the frequencies is sufficiently large. Here we define the effective scattering opacity at a wing frequency x by $\tau_e(x)$. At the first scattering of Ly α photon with the expanding supershell, the effective optical depth should be measured at $x_0 + x_{\text{exp}}$, i.e. $\tau_e(x_0 + x_{\text{exp}})$. Here we consider an input frequency $x_0 = 0$, for simplicity. Note that $x_{\text{exp}} < 0$. If $\tau_e(x_0 + x_{\text{exp}}) \gg 1$, a back-scattering occurs at the wing frequency. Then, the back-scattered photons are redshifted to the frequency $x = x_0 + x_{\text{exp}}$, and they will scatter in the other part of the supershell along the back-scattered direction. If the supershell in that direction is optically thin, then those back-scattered photons can escape freely to form a prominent peak. In fact, that part of the supershell is also receding with respect to the back-scattered photons, and so the effective opacity now becomes $\tau_e(x_0 + 2x_{\text{exp}})$. The opacity at this frequency is even smaller than that of previous scattering, and the escape probability

increases. Hence some photons escape the system and form the first peak at $x = x_0 + x_{\text{exp}}$. The photons reflected into slant directions are redshifted by an amount smaller than those to the normal direction, and the optical depths in those direction becomes larger. Hence the escape probability of those photons become smaller than that of photons in the normal direction. These photons contribute to the broadening of each peak. It is also noticeable in the figure that the primary peak is not well matched with x_{exp} , because its blue part is eroded by the scattering of very thick supershell whose scattering centre is located at $x = -x_{\text{exp}}$ in the figure.

Ly α photons repeat the above-mentioned back-scatterings until τ_e becomes small enough to permit most of the photons to escape the system. We see that photon's effective scattering frequency at the N -th back-scattering is given by $2(N - 1)x_{\text{exp}}$, where $N > 1$. The frequency of photons escaping associated with N -th back-scattering is given by $(2N - 3)x_{\text{exp}}$. When $N = 1$, the situation is special, because the source is at rest. In this case, each frequency is x_{exp} and 0, respectively.

We illustrate in Figure 3 how the effective opacity of successive back-scatterings varies, where we consider photons scattering back and forth along a diameter for simplicity. The effective frequencies of Ly α photons successively change, as is drwan by the vertical dotted lines in the figure. The numbers in the box for each dotted line refers to the order of back-scatterings denoted by N . Let us consider the case for $\tau_0 = 10^6$ which corresponds to the case in Figure 2. We can see that the effective opacity for $N = 1$ is very large, and so most of Ly α photons are back-scattered. This means that there is a little amount of transmitted flux with $x = 0$. The second or $n = 2$ back-scattering happens at wing frequencies much further away from the $N = 1$ frequency, and so the escape probability is enhanced, but it is still not large enough for most photons to escape the system. However, the emission peak forms at $x = x_{\text{exp}}$, because the flux of incident Ly α photons is very large. In the next turn with $N = 3$, the second peak at $x = 3x_{\text{exp}}$ forms due to the process similar to the $N = 2$ case. When $N = 4$, we expect that the other peak, but it appears very weak because most Ly α photons have already escaped from the system. From then on the effective opacities for the following back-scatterings are sufficiently small, but photons have been already exhausted. So no peaks at the higher frequencies appear in the emergent spectrum, as shown in Figure 2. We can summarize mathematically these explanation as follows.

$$I_1(0) = I_0 f_T(x_{\text{exp}}) \simeq 0, \tag{8}$$

$$\begin{aligned}
I_2(x_{\text{exp}}) &= I_0 [1 - f_{\text{T}}(x_{\text{exp}})] f_{\text{T}}(2x_{\text{exp}}) \\
&= I_0 f_{\text{R}}(x_{\text{exp}}) f_{\text{T}}(2x_{\text{exp}}),
\end{aligned} \tag{9}$$

$$I_3(3x_{\text{exp}}) = I_0 f_{\text{R}}(x_{\text{exp}}) f_{\text{R}}(2x_{\text{exp}}) f_{\text{T}}(4x_{\text{exp}}), \tag{10}$$

$$I_4(5x_{\text{exp}}) = I_0 f_{\text{R}}(x_{\text{exp}}) f_{\text{R}}(2x_{\text{exp}}) f_{\text{R}}(4x_{\text{exp}}) f_{\text{T}}(6x_{\text{exp}}), \tag{11}$$

and so on. Generally

$$\begin{aligned}
I_N ([2N - 3]x_{\text{exp}}) &= I_0 f_{\text{R}}(x_{\text{exp}}) \\
&\quad \prod_{n=2}^{N-1} f_{\text{R}}([2n - 2]x_{\text{exp}}) \cdot f_{\text{T}}([2N - 2]x_{\text{exp}}),
\end{aligned} \tag{12}$$

where the transmitted fraction (f_{T}) and the reflected fraction (f_{R}) are approximately described in Eq.(2.32) and Eq.(2.33), respectively of Neufeld (1990). Here I_0 is the input flux, and I_N is the flux associated with the N -th back-scattering.

In order to see how much emergent Ly α photons are affected by dust extinction, we calculate the total path length of the emergent photons through the medium. Here we adopt $N_{\text{HI}} \simeq 2 \times 10^{20} \text{cm}^{-2}$, $b = 40 \text{ km s}^{-1}$, and $V_{\text{exp}} \simeq 300 \text{ km s}^{-1}$. We also assume that dust is uniformly distributed in the supershell.

In Figure 4 we show the spectral distribution of both the total path length of Ly α photons in the supershell (τ_{d}) and the total number of scatterings (N_{scat}). The latter represented by solid circles in the inset is depicted in logarithmic scale, and shows clearly two groups. One group is located at the upper domain with $\log_{10} N_{\text{scat}} \sim 6$, and they are photons having experienced excursions. The rest in the lower part with $\log_{10} N_{\text{scat}} \approx 1$ are those having escaped by a number of back-scatterings.

The crosses represent, in units of τ_0 , the total path length along which a Ly α photon traversed in the supershell. We can see in the figure that most of emergent photons escape by back-scattering, which can be inferred from the small number of scatterings. It is also noticeable that the total path lengths are very diverse in the spectral distribution and most of photons traverses rather short path. Since there is no frequency-dependence in path lengths except for a weak trend of monotonous increases, the redder peaks in emergent profiles from dusty media can be destroyed at most a little bit more than the bluer peaks. This is puzzling because all the observed Ly α profiles shows single peak which must be the $N = 2$ peak in our calculations. The solution of this puzzle may lie in the spatial distribution of dust in the system. If the inner radius of the dust shell is smaller than that of neutral hydrogen, the

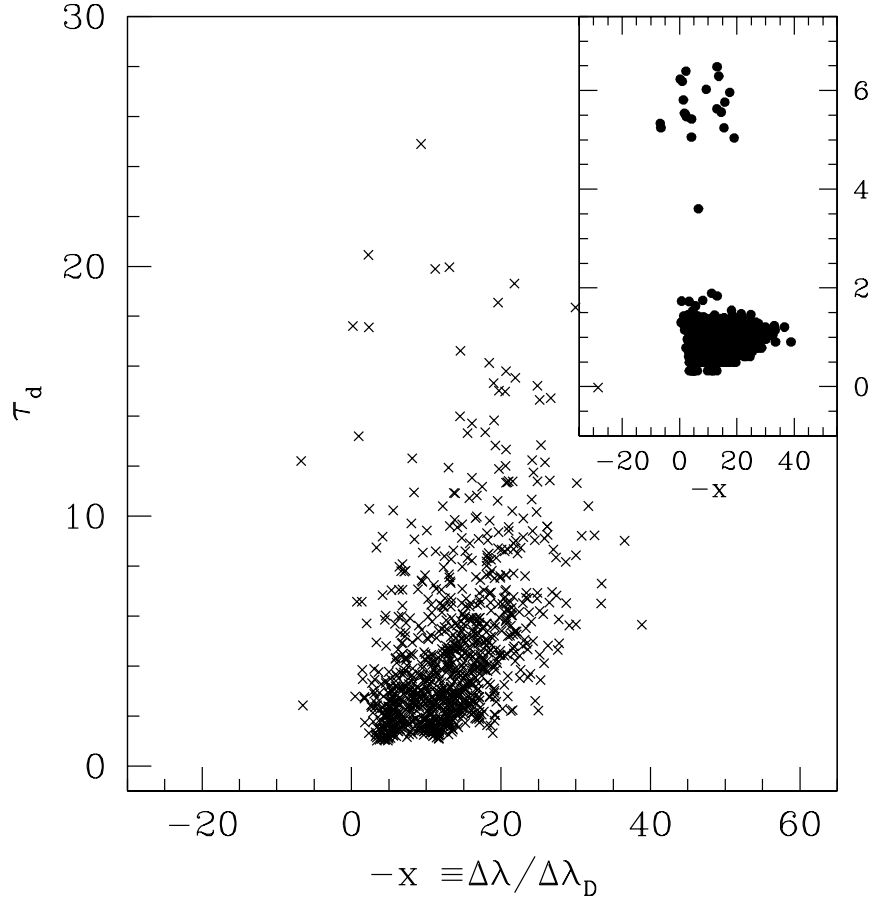


Figure 4. Spectral distribution of the number of scatterings (N_{scat}) denoted by solid dots and the total path lengths (τ_d) represented by crosses. The calculation is performed for a model with the line-centre optical depth $\tau_0 = 8.3 \times 10^6$, the expansion velocity in units of thermal width $x_{\text{exp}} = -7.65$, and the FWHM of input profile $\Delta x = 2$.

dust extinction of the higher order peak can increase. We are now undertaking this subject, and the results will be published in the forthcoming paper.

4 DEPENDENCE ON THE PHYSICAL PARAMETERS

The emergent profiles depends on a few parameters of scattering medium in our model. First of all, the turbulence is out of our interest, because they are constrained by observations and the emergent profile is dominantly formed by kinematics of the supershell in our case. Hence here we investigate how the Ly α peaks depend on the optical depths and the expansion velocity of the supershell.

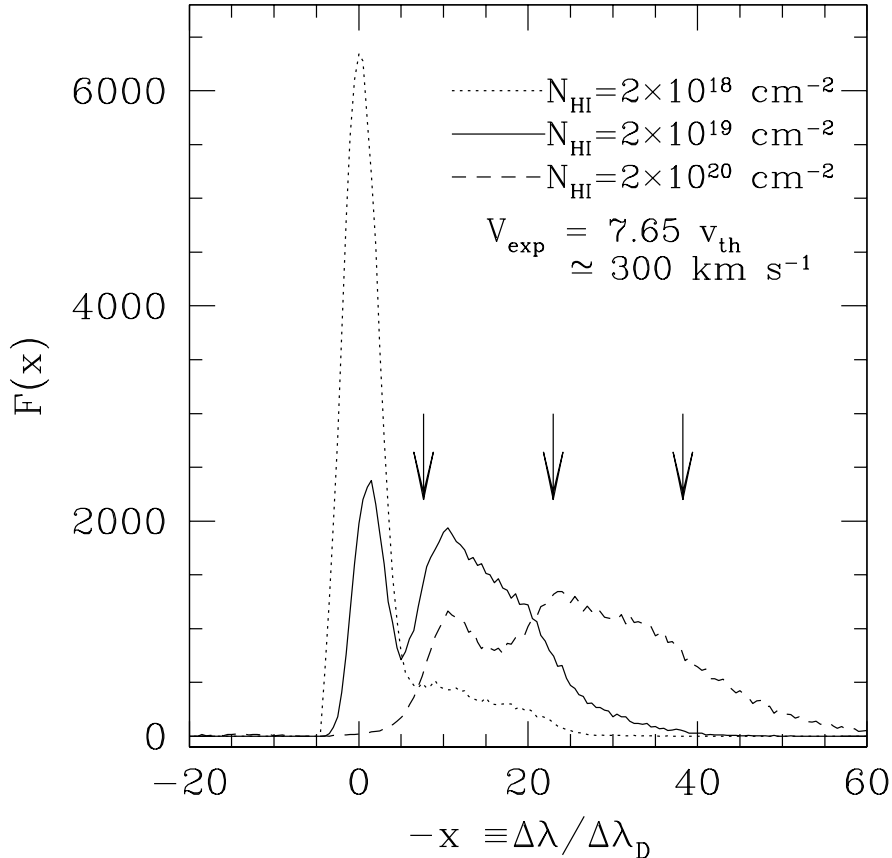


Figure 5. Emergent Ly α profiles for three cases in which the supershells have different line-centre optical depths but their expansion velocities are fixed. The parameters are given in the box, and the arrows refers to the location of possible emission peaks formed by back-scatterings.

4.1 Effects of supershell's opacity

We present in Figure 5 the emergent profiles for a few cases with different line-centre optical depths, where the expansion velocity of the supershell is fixed to be $x_{\text{exp}} = -7.65$. The FWHM of input profiles is also set to be $\Delta x = 2$, and the Doppler parameter of the supershell is set to be $b = 40 \text{ km s}^{-1}$. The supershell is assumed to have no dust, and the number of input photons are set to be equal for each calculation or $N_{\text{ph}} = 80,000$. The arrows in the figure represent the peaks corresponding to x_{exp} , $3x_{\text{exp}}$, and $5x_{\text{exp}}$. When the opacity of the supershell is not sufficiently large ($N_{\text{HI}} = 2 \times 10^{18}$, 2×10^{19}), the input photons are transmitted without scatterings and the peak at $x \simeq 0$ forms, whose FWHM increases by a small amount compared to that of input profile. We can see in the figure that the back-scattered photons form the primary peak at $x \simeq x_{\text{exp}}$, the secondary peak at $x \simeq 3x_{\text{exp}}$, and

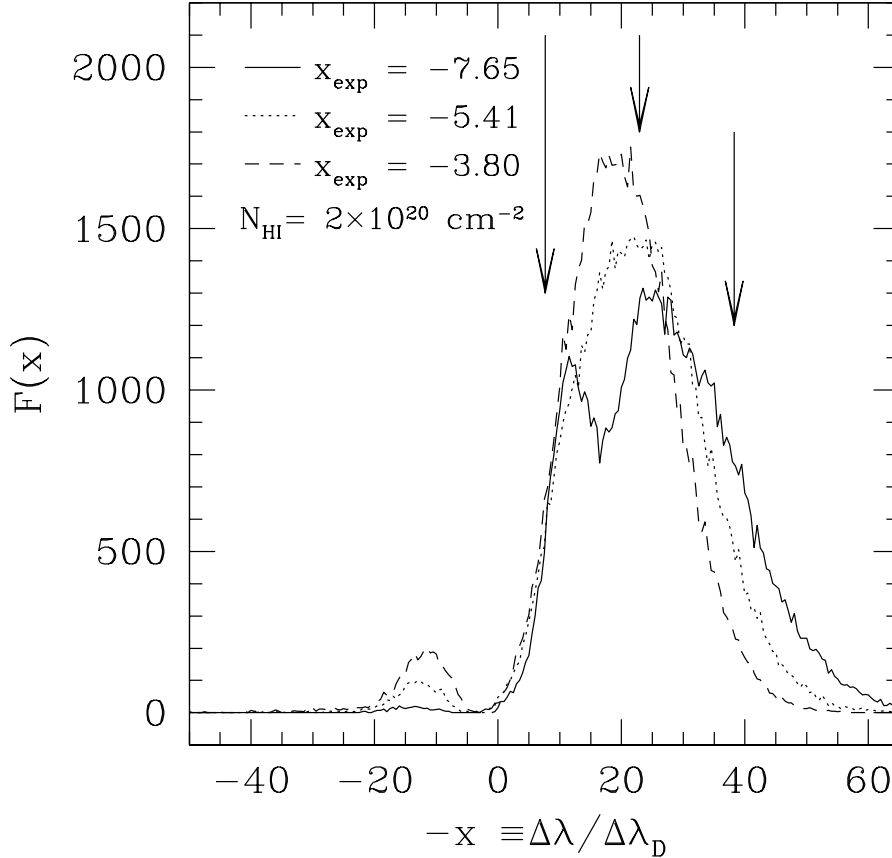


Figure 6. Emergent profiles of Ly α for several cases with different expansion velocities. The horizontal axis refers to the wavelength in units of thermal width, and the vertical axis represents the number flux of emergent profiles. We assume that the input profiles have the same Gaussian input profile with $\Delta x = 2$ FWHM and the same number flux of photons or 80,000. The column density of neutral hydrogen in the supershell is also fixed or $N_{\text{HI}} = 2 \times 10^{20} \text{ cm}^{-2}$. The meaning of each line is shown in the box, and the arrows represent the frequencies for the primary, secondary, and tertiary peaks for $x_{\text{exp}} = -7.65$.

the tertiary peak at $x \simeq 5x_{\text{exp}}$. As the opacity of the supershell decreases, the peaks at higher frequencies disappear accordingly. We have explained the mechanism of those variations in the previous section.

4.2 Effects of Kinematics

We also investigate the effects of the expansion velocity of the supershell. The results of Monte Carlo calculations are shown in Figure 6. We can see that the emission peaks gradually merge into a single peak as $|x_{\text{exp}}|$ decreases. This is because the supershell behaves like a spherical medium which is static with respect to the Ly α source as $|x_{\text{exp}}| \rightarrow 0$. In an extremum with $|x_{\text{exp}}| < 1$, the emergent profiles will have symmetric double peaks which is

same to those given in Ahn et al. (2002). If $|x_{\text{exp}}|$ is much larger than unit, then we can see the emission peaks of back-scattered photons in the emergent profile. However, as $|x_{\text{exp}}| \rightarrow 1$, the frequency gaps between those peaks become close, and they eventually mixed up to be a single broad peak. We can also expect a heavy extinction for small $|x_{\text{exp}}|$ cases.

It is also noticeable that the similar problem for the contraction supershell has a exact mirror-symmetry to the expanding supershell. Hence it is evident that we obtain the profiles to the origin $x = 0$ for the contracting case.

5 SUMMARY

We have investigated the formation of P-Cygni type Ly α by a supershell surrounding a star-forming region and outflowing in a bulk manner with expansion velocities of $V_{\text{exp}} \sim 100 - 300 \text{ km s}^{-1}$. We have modified the Monte Carlo code developed in the previous paper (Ahn et al. 2001), and studied in detail the Ly α line transfer in the expanding supershell consists of neutral hydrogen gas. The Ly α line-centre optical depth of the supershell is very large and of order $\tau_0 \sim 10^5 - 10^7$. Its turbulence motion is assumed to be about 40 km s^{-1} in accordance with observations.

We found that the back-scatterings play a crucial role in the formation of asymmetric Ly α profiles. Most of Ly α photons escape the system efficiently through back-scatterings. Whenever it is scattered back by the expanding supershell, photon's frequency is redshifted successively. This process promotes the redshift of Ly α photons. It is also naturally expected that the collapsing supershell promotes blueshift of Ly α photons, and the emergent profile for that case is simply mirror-symmetric to that of the expanding case. The emission peak formed by the N -th back-scattering with the supershell has a frequency of $(2N - 3)x_{\text{exp}}$, where $N > 1$. The number of peaks and their relative flux ratios in emergent profiles are determined by the interplay between the line-centre optical depths and the expansion velocities of supershells.

Recently optical nebular lines of about a dozen of Lyman break galaxies have been obtained by using near-IR spectrographs and large telescopes (Pettini et al. 2001; Teplitz et al. 2000a; Teplitz et al. 2000b). The Ly α spectra of a large number of primeval galaxies can be found in the literature (Steidel et al. 1996; Steidel et al. 1999; Lowenthal et al. 1997; Frye et al. 2002), which are reviewed in Stern & Spinrad (1999). Their UV spectra and Ly α emission lines show similar characteristics to those of nearby starburst galaxies. Their P-Cygni type

Ly α emission lines are always accompanied by nebular lines blueshifted with respect to Ly α . We have showed that these asymmetric Ly α can be formed by back-scatterings of Ly α photons by an expanding supershell.

The quantitative measurement of star-formation rates of starburst galaxies is one of the most crucial issues in modern cosmography. It is suggested that the expansion of surrounding media can help Ly α photons escape the star-forming regions more freely. In light of our works, it is very interesting to see that nearly all the observed P-Cygni type Ly α emissions from starburst galaxies do not show any higher order peaks which are formed by back-scatterings. This can certainly be attributed to dust extinction. However, it is very subtle problem if we want to quantify the escape fraction of Ly α photons for the case of the dusty and expanding supershell. Hence, we believe that very careful consideration of both abundance and spatial distribution of dust is needed to establish a realistic model describing the star-forming activity in starburst galaxies whether it is nearby or primeval. We are now undertaking this topic, and its results will be reported in a forthcoming paper.

ACKNOWLEDGMENTS

This work was done as a part of doctoral dissertation of SHA at the School of Earth and Environmental Sciences of Seoul National University financially supported by Brain Korea 21 of the Korean Ministry of Education. Also this work is completed with financial support of Korea Institute for Advanced Study, which is gratefully acknowledged. HML was supported by KOSEF Grant No. R01-1998-00023.

REFERENCES

- Adams, T. 1972, ApJ, 174, 439
Ahn, S. -H. & Lee, H. -W. 1998, astro-ph/9801031
Ahn, S. -H. 2000, ApJ, 530, L9
Ahn, S. -H., Lee, H. -W., & Lee, H. M. 2000, Jour. of Korean Ast. Soc., 33, 29
Ahn, S. -H., Lee, H. -W., & Lee, H. M. 2001, ApJ, 554, 604
Ahn, S. -H., Lee, H. -W., & Lee, H. M. 2002, ApJ, 567, 922
Charlot, S. & Fall, S. M. 1993, ApJ, 415, 580
Frye, B., Broadhurst, T., & Benítez, N. 2002, ApJ, in press, astro-ph/0112095
González Delgado, R. M. et al. 1998, ApJ, 495, 698
Harrington, J. P. 1973, MNRAS, 162, 43
Kunth, D., Mas-Hesse, J. M., Terlevich, E., Terlevich, R., Lequeux, J., & Fall, S. M. 1998, A&A, 334, 11
Lee, H. -W. & Ahn, S. -H. 1998, ApJ, 504, L61

- Lowenthal J. D. et al. 1997, *ApJ*, 481, 673
- Marlowe, A., Heckman, T., Wyse, R. 1995, *ApJ*, 438, 563
- Martin, C. 1998, *ApJ*, 506, 222
- Neufeld, D. A. 1990, *ApJ*, 350, 216
- Pettini, M., Shapley, A. E., Steidel, C. C., Cuby, J. -G., Dickinson, M., Moorwood, A. F. M., Adelberger, K. L., & Giavalisco, M. 2001, *ApJ*, 554, 981
- Steidel, C. C., Giavalisco, M., Pettini, M., Dickinson, M., & Adelberger, K. L. 1996, *ApJ*, 462, 17
- Steidel, C. C., Adelberger, K. L., Giavalisco, M., Dickinson, M., & Pettini, M. 1999, *ApJ*, 519, 1
- Stern, D. & Spinrad, H. 1999, *PASP*, 111, 1475
- Teplitz, H. I., McLean, I. S., Becklin, E. E., Figer, D. F., Gilbert, A. M., Graham, J. R., Larkin, J. E., Levenson, N. A., & Wilcox, M. K. 2000, *ApJ*, 533, L65
- Teplitz, H. I., Malkan, M. A., Steidel, C. C., McLean, I. S., Becklin, E. E., Figer, D. F., Gilbert, A. M., Graham, J. R., Larkin, J. E., Levenson, N. A., & Wilcox, M. K. 2000, *ApJ*, 542, 18
- Thommes, E., Meisenheimer, K., Fockenbrock, R., Hippelein, H., Roeser, H.-J., & Beckwith, S. 1998, *MNRAS*, 293, L6